

macerated with 40% hydrofluoric acid for two days. Occasional stirring and shaking helped to extract the pollen grains from the rock matrix. The pollen remains were screened by using 325 and 400 size mesh sieves. Individual pollen grains were picked up, mounted in polyvinyl alcohol and studied under light and scanning electron microscopes.

The pollen grains are oval-elliptical in shape. Most of them are monosulcate-trichotomosulcate type with distinct sulcus; but inaperturate condition is also noticed (Figure 1c-h). They are 62–95 μm in size. The exine is 3–4 μm thick, uniformly and finely reticulate, coarser at the periphery and faint towards the centre. The foveolae are relatively small when compared to the thick winding muri forming retipilate structure at the periphery (Figure 1i, j).

The majority of the pollen grains recovered after maceration represents a single morphological taxon, although there has been a considerable variation in the aperture, from inaperturate, monosulcate to trichotomosulcate. Large size, inaperturate, monosulcate to trichotomosulcate condition, finely reticulate exine and relatively small foveolae compared to thick winding muri are the characteristics of the recovered pollen grains and suggest an affinity with Liliaceae. Among the Liliaceae itself, there is a variation in the aperture and exine ornamentation. Therefore, it is very difficult to assign the fossil pollen grains to the known genera in Liliaceae at present. However, the size of the grains and exine ornamentation patterns are comparable to *Hemerocallis*, *Asphodelus* and *Lilium*⁵. The exact affinity can be ascertained after studying comparable material under SEM.

Sporae dispersae of such type of pollen grains have been described as *Matanomadhiasulcites* from the Palaeocene–Oligocene rocks of India, Africa and America. Strictly speaking, *Matanomadhiasulcites* shares an affinity with Liliaceae/Agavaceae rather than Annonaceae.^{6,7} In our opinion also, liliaceous affinity is more appropriate as the pollen grains are considerably large with a tectate exine. A reinvestigation of the type species and other species assigned to *Matanomadhiasulcites* is warranted in order to ascertain the affinity.

ACKNOWLEDGEMENTS. We are grateful to Mrs. M. M. Harley, Kew Botanical Gardens, England; Dr. K. Ambwani, Birbal Sahni Institute of Palaeobotany, Lucknow and Dr (Mrs.) M. Chaturvedi, National Botanical Research Institute, Lucknow for their critical comments.

Received 4 June 1993; revised accepted 19 July 1993

Deposition of Mn–Cu–Ni-enriched sediments during Glacial period in the Central Indian Basin

D. V. Borole

National Institute of Oceanography, Dona Paula, Goa 403 004, India

Two siliceous sediment cores collected from the Central Indian Basin have been analysed for organic carbon, biogenic silica, Al, Mn, Ni and Cu content. The concentrations of Mn, Cu and Ni showed one order of magnitude variation (an enrichment by a factor of 20) down the core, with a pronounced maximum at depths of 78 cm and 26 cm, corresponding to 390 ± 80 and 320 ± 60 kyr BP, respectively. The depthwise variation of Mn content matches closely that of cold water subtropical fauna, with both the parameters showing inverse relationship with organic carbon. The observed variations are due to changes in the palaeo-oceanographic conditions.

THE development of the abyssal plains of the Central Indian Basin (CIB) has been attributed to turbidity currents of the Ganges Fan, which disperse sediments to far south^{1,2}. The bathymetric and tectonic studies in this region reveal the presence of several abyssal, conical hills covered with pumice^{3,4}. These features are suggestive of submarine volcanic activity during the past.

Siliceous matter dominates these (Quaternary) sediments of the northeastern regions of CIB, with traces of pelagic clay⁵. Interestingly, terrigenous clay occupies the northern (distal end of the Bengal Fan) part of CIB. Calcareous ooze prevails in the shallow regions, with their abundance decreasing with increasing water depth before becoming sparse due to dissolution of CaCO_3 (ref. 1).

It is well known that the deeper waters of CIB come under the influence of a pronounced front, with the

1. Daghlian, C. P., *Bot. Rev.*, 1981, 47, 517–555.
2. Lakhapal, R. N., Prakash, U. and Bande, M. B., *Palaeobotanist*, 1982, 30, 316–324.
3. Tidwell, W. D. and Parker, L. R., *Rev. Palaeobot. Palynol.*, 1990, 62, 79–95.
4. Couper, R. A., *N. Z. Geol. Surv. Palaeontol. Bull.*, 1953, 22, 1–77.
5. Nair, P. K. K. and Sharma, M., *J. Palynol.*, 1965, 1, 38–61.
6. Kar, R. K., *Palaeobotanist*, 1985, 34, 1–249.
7. Venkatachala, B. S., Caratini, C., Tissot, C. and Kar, R. K., *Palaeobotanist*, 1989, 37, 1–25.

characteristic hydrochemical structure at 10°S latitude separating the reversing monsoon and the subtropical gyres^{6, 7}. Apart from this, the waters of CIB indicate the presence and northward spread of Antarctic Bottom Water (AABW) from the Weddell sea^{7, 8} across the low-latitude saddles over Ninety East Ridge.

Geochemical studies of deep-sea sediments help in identifying metal sources and sinks, apart from providing a clue to their removal mechanism from the overlying water column^{9, 10}.

Earlier studies on the geochemistry of the sediments of CIB region are confined either to surface sediments¹ or to shorter cores¹¹ (~ 300 kyr BP) and relate to the surface (at ~ 25 cm or ~ 300 kyr BP) remobilization of metals^{12, 13}.

This article discusses metal enrichment in longer, deep-sea sediment cores (F200B and F88B) from CIB in the light of variations in organic carbon and

biogenic silica, which are considered as the tracers of palaeo-productivity^{14, 15}. The significance of Mn, Cu and Ni enrichment layer at 20–80 cm (~ 390–320 kyr BP) below the sediment–water interface of these sediment cores is highlighted.

The concentration of various elements (e.g. Al, Mn, Ni and Cu) in the bulk sediment were determined by flame atomic absorption spectrophotometry. Following the standard procedures^{16, 17}, measurements were made on USGS reference rock W-2, keeping the coefficient of variation at ± 5%, to cross-check the results. Organic carbon¹⁸ was estimated to a precision of ± 0.01%.

The observed chemical composition of the sediment cores (Figures 1 and 2) at depths of 76 cm (F200B) and 26 cm (F88B) depicts a marked Cu and Ni enrichment equivalent to nearly 20 times the concentration at the sediment–sea-water interface.

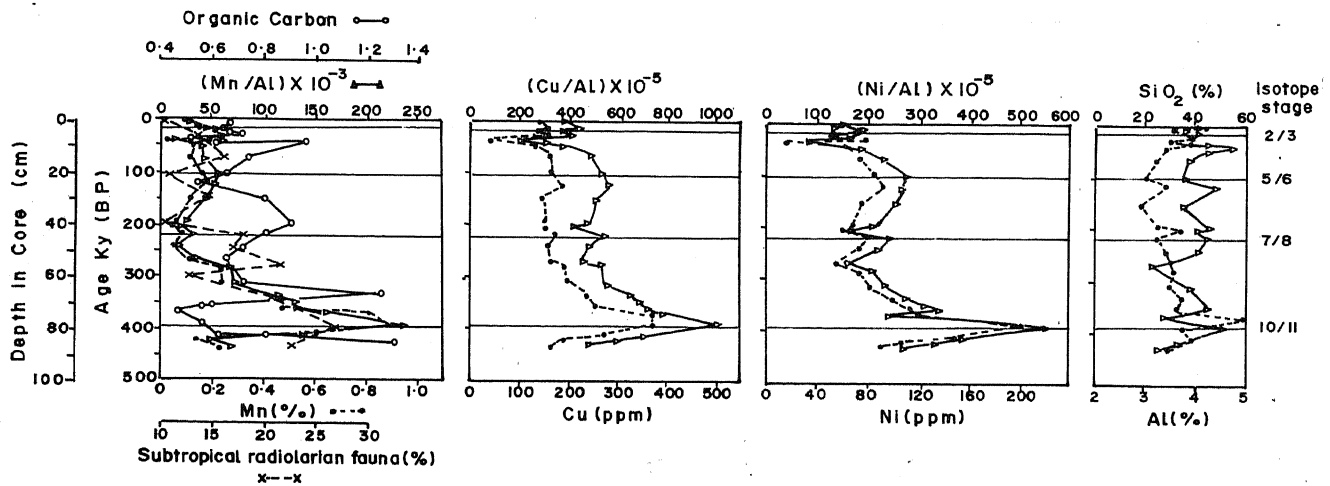


Figure 1. Variation of metal concentration (dotted lines bottom scale) and metal/Al (solid lines top scale) ratio of core F200B. Also shown is the average abundance of subtropical fauna, organic carbon, biogenic silica (triangles top scale) and Al (filled circles bottom scale). Isotopic stages are marked based on ²³⁰Th_{ex} chronology²⁷ and radiolarian stratigraphy³³.

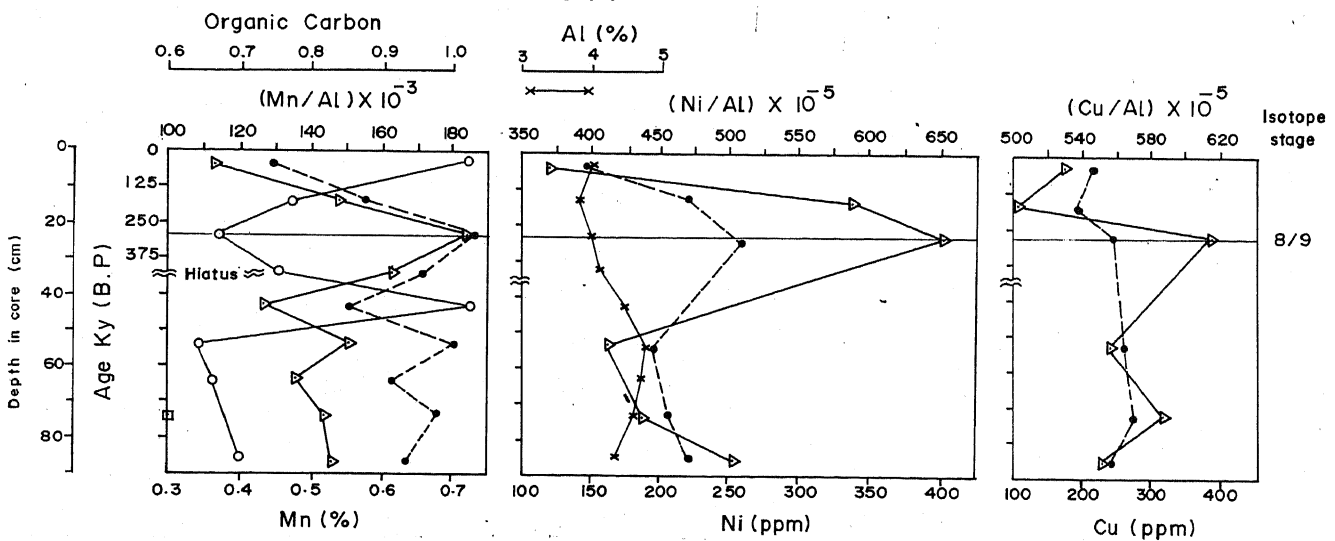


Figure 2. Variation of metal concentration and metal/Al ratio, organic carbon, and Al for core F88B.

RESEARCH COMMUNICATIONS

Table 1. Details of the core samples from Central Indian Basin²⁷

Sample code	Location		Water depth (m)	Sedimentation rate (cm/kyr)	Remarks
	Lat. (°S)	Long. (°E)			
F200B	12.0	76.5	5450	0.2	Undisturbed, 90 cm long Benthos core. Radiolarian ooze contains volcanic glass ³³ shards. Five volcanic ash beds at 0-15, 20-30, 46-50, 72-76 and 82-86 cm level.
F88B	12.7	77.0	5430	0.08	Undisturbed, 86 cm long benthos Boomerang core. Radiolarian ooze with volcanic ash beds at 0-5, 20-25 and 30-35 cm levels. A hiatus reported for a period of ~300 kyr from 0.4 to 0.7 myr at 35/40 cm

Similar observations of Mn enrichment at surface and subsurface levels of sediment cores from pelagic environment have been documented earlier^{9, 19, 20}. The fluctuating nature of these concentrations has been attributed to (i) post-depositional diagenesis, (ii) tectonic effects, e.g. submarine volcanism and hydrothermal activity, (iii) effects of climate variation, or (iv) influx of fine-grained, fluvial sediments enriched in these metals and their subsequent leaching by sea water.

Importance of Mn as a model element for studies of redox processes in the sea^{21, 22} needs no special mention as it is one of the important electron acceptors in organic carbon oxidation during the early diagenesis²³. Hence, near the sediment-water interface, Mn is mobilized as dissolved Mn²⁺ under reducing conditions, and immobilized as MnO_x (where x ranges from 1.7 to 1.9, for example)²⁴ under oxic conditions.

Mn responds (sensitive) to palaeo-oceanographic changes. Mn enrichment due to changes in the concentration of the overlying water column—due mainly to palaeo-climatic events, e.g. increase in the flow of AABW during glacial period^{25, 26}—and changes associated with phases of transition from glacial to interglacial periods²⁰ have been reported for the sediments of the Atlantic and Pacific regions.

What must have contributed to the enrichment of Mn and other transition elements could become clear when the tectonic effects and palaeo-productivity changes also are examined in detail.

Depthwise distribution of Al (predominantly terrigenous in origin) indicates differential inputs during the past. The prominent peaks at 0-15, 20-30, 46-50, 72-76 and 82-86 cm (Figure 1) coincide with the peaks reported for glass shards (Table 1). In order to express metal concentrations on the basis of clay content, we examined the absolute concentrations and their normalized values with respect to Al (metal/Al) (Figures 1 and 2). Such a normalization with respect to Al takes into account also the variation of clay fractions and the changes in the intensity of weathering, which would ultimately lead to material deposition in the sea.

Profiles of Mn, Ni and Cu contents of core F200B display two secondary maxima (at 23-25 and 41-46 cm) well above the pronounced maxima at about 76-80 cm (Figure 1). One can notice a relative increase in biogenic silica at this level in contrast to organic carbon, which exhibits a decrease only at 23-25 cm. Based on sedimentation rates²⁷ for these cores (Table 1), these layers correspond approximately to 115-125 kyr, 205-230 kyr, and 380-400 kyr, respectively (Figure 1). Similarly, Mn, Cu and Ni from core F88B present one pronounced maxima at 21-26 cm, corresponding to 265-325 kyr B.P. These, in a way, correspond to interglacial and glacial periods having isotope stages in the range 5-11.

Based on geochronological studies, this basin was considered as one region subjected to winnowing by bottom currents²⁷. These studies provided evidence in the form of unsteady sedimentation while examining the profiles of ²³⁰Th_{ex} and the variations in the sedimentation rates (0.08-0.43 cm kyr⁻¹).

Despite variable sedimentation rates, the enrichment of Mn and other transition elements (Figures 1 and 2) in both the cores point to a phenomenon common to physicochemical changes around 325-400 kyr BP.

One plausible cause for the subsurface Mn enrichment could be that Mn, Cu and Ni are scavenged by the micronodules in the sediments²⁸. However, in the present cores, micronodules were scanty with sparse distribution. In siliceous environments micronodules decrease in size and abundance with depth^{12, 29, 30}. A microscopic examination of the coarse fraction of these sediments reveals the absence of dissolution features—an observation supported by clean radiolarian tests—thereby discarding the possibility of having a coat of Mn on the carbonate shells, as reported in ref. 31.

This leaves two possibilities for the enrichment of Mn and other transition elements—namely, tectonic effects and palaeo-productivity and the concurrent redox changes. The presence of glass shards in the ash beds at five depths (F200B, F88B, Table 1)—related to underwater volcanic activity—higher as well as variable Fe/Mn ratios, and proximity to the chain of

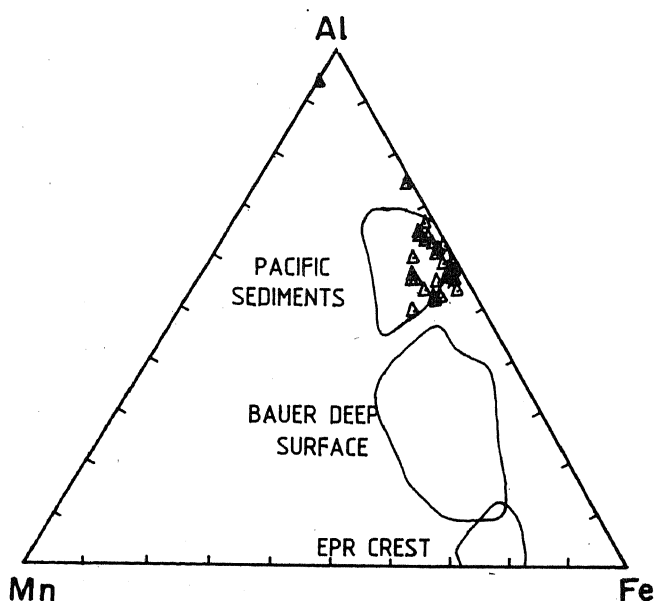


Figure 3. Ternary diagram for Al, Fe and Mn for core F200B and F88B.

seamounts in the locality may suggest submarine volcanism during Quaternary period to be one of the possible causes for Mn enrichment. However, there is a mismatch or lack of significant correlation between the peaks in depthwise concentration of Mn (F200B 23–25, 41–46, 76–80 cm) and the ash layers. As such, it does not lend support to submarine volcanism as a cause for this observed enrichment. Examination of the ternary diagram³² (Figure 3) also rules out hydrothermal activity as a possible cause for the observed enrichment.

At this stage, the close correspondence in the peaks of Mn and the subtropical radiolarian fauna deserves attention as the latter responds better to climatic changes. Simultaneously, the fact that the cold water fauna bears an inverse relation to organic carbon could now be recalled.

The depthwise variation of Mn concentration in the sediment core (F200B) and the percentage abundance of subtropical radiolarian recurrent groups⁸, consisting of six conspicuous cooler water species from the Indian Ocean, are presented in Figure 1. Mn distribution broadly resembled the variation in subtropical faunal content. The principal peak (~0.9%) in Mn concentration (uncorrected for biogenic components) coincides with the highest (~26%) abundance of subtropical fauna. This explains the observed Mn content and subtropical fauna with changes in the overlying water column. The Mn content and the subtropical fauna shows a trend synchronous with climatic fluctuations. However, the cold water fauna is

inversely related to organic carbon. Core F88B shows definitely an inverse relation between the two. The presence of a cold water taxa provides evidence for the cold period in core F88B. Evidence of strong bottom water currents (largely comprised of AABW), substantiated by the presence of extended hiatus between 360 to 400 kyr BP, also exists.

The organic carbon and Mn profiles for cores F200B and F88B (Figures 1 and 2) appear to be a mirror image of each other and bear an inverse relation. The Mn distribution in this region may be a result of the reductive dissolution effects originating from a non-steady-state diagenesis. Towards the end of the glacial period, the organic carbon attains peak values. As the glacial maximum is reached, organic carbon decreases to a minimum (due to efficient decomposition) while Mn content increases (due to enhanced oxidation) because of the lowered temperature and increased oxygen dissolution (Figures 1 and 2).

Thus, during the glacial period, the higher dissolved oxygen favours the decomposition of organic carbon, leading to a minimum, while the higher preservation of Mn contributes to a maximum for Mn. When pore water Mn^{2+} migrates upwards, it is oxidized to Mn^{4+} and precipitated within the surface layer. Thus, cold water movements in this area promote oxidizing conditions, under which Mn^{2+} in the water precipitates as Mn^{4+} ('oxidative scavenging effect'), leading to the observed enrichment of total Mn.

Similar observations of metal-rich layers have been reported in the literature in a number of deep-sea sediments at, or just below, the Glacial-Holocene transition. The enrichment can be explained in terms of the concept^{34, 35} of progressive oxidation front moving into the sediment following the change from glacial to interglacial conditions, wherein the depth of oxidant penetration from sea water hovering around a near-fixed depth and balanced by the reductant counter flux of Mn^{2+} and Fe^{2+} from the reducing sediments below.

1. Nath, B. N., Rao, V. P. and Becker, K. P., *Mar. Geol.*, 1989, **B87**, 301–303.
2. Kolla, V. and Kidd, R. B., in *The Ocean Basins and Margins, The Indian Ocean* (eds Nairn, A. E. M. and Stehli, F. G.), Plenum, New York, 1982, pp. 6, 1–45.
3. Kodagali, V. N., Kameshraj, K. A., George, P. and Jaishankar, S., *Int. Hydrol. Rev.*, 1992, **69**, 143–150.
4. Iyer, S. D. and Sudhakar, M., *Deep Sea Res. I*, 1993, **40**, 1123–1129.
5. Udintsev, G. B., Fisher, R. L., Kanaeo, V. F., Laughton, A. S., Simpson, E. S. W. and Zhiv, D. I., *Geological-Geophysical Atlas of the Indian Ocean*, Pergamon, 1975, p. 151.
6. Wyrtki, K., in *Physical Oceanography of the Indian Ocean* (ed. Zeitschel, B., Springer, Berlin, 1973, 18–36.
7. Warren, B. A., *J. Mar. Res.*, 1982, **40**, 823–860.
8. Johnson, D. A. and Nigrini, C., *Mar. Micropaleontol.*, 1982, **7**, 237–287.

9. Chester, R., *Marine Geochem.*, Academic Division of Unwin Hyman Ltd, London, 1990, p. 698.
10. Broecker, W. S. and Peng, T. H., in *Tracers in the Sea*, Lamont Doherty Geological Observatory Press, Columbia University, New York, 1982, p. 690.
11. Nath, B. N. and Mudholkar, A. V., *Mar. Geol.*, 1989, **86**, 57-66.
12. Roy, S., Dasgupta, S., Mukhopadhyay, S. and Fukuoka, M., *Mar. Geol.*, 1990, **92**, 269-283.
13. Pattan, J. N. and Mudholkar, A. V., *Chem. Geol.*, 1990, **85**, 171-181.
14. Schramm, C. T., MS Thesis, University of Rhode Island, 1983, p. 127.
15. Muller, P. J., Erlenkeuser, H. and Grafenstein, V. R., in *Upwelling: Its Sediment Record*, Part B (eds Thiede, J. and Suess, E.), Plenum, New York, 1983, pp. 365-398.
16. Borole, D. V., Sarin, M. M. and Somayajulu, B. L. K., *Indian J. Mar. Sci.*, 1982, **11**, 51-62.
17. Sarin, M. M., Borole, D. V. and Krishnaswami, S., *Proc. Indian Acad. Sci. (Earth and Planet. Sci.)*, 1979, **88A** (Part II, 2), 131-154.
18. El Wakeel, S. K. and Riley, J. P., *J. Conseil Int. l'Explor. Mer*, 1957, **22**, 180-183.
19. Finney, B. P., Lyle, M. W. and Heath, G. R., *Paleoceanography*, 1988, **3**, 169-189.
20. Mangini, A., Eisenhauer, A. and Walter, P., *Paleoceanography*, 1990, **5**, 811-821.
21. Finney, B. P., Ph D thesis, Oregon State University, Corvallis, 1987, p. 195.
22. Johnson, K. S., Berelson, W. M., Coale, K. H., Coley, T. L., Elord, A. V., Fairey, W. M., Kilgore, H. D. Iams Tammy and Nowicki, J. L., *Science*, 1992, **57** 1242-1246.
23. Froelich, P. N., Klinkhammer, G. P., Bender, M. L., Luedtke, N. A., Heath, G. R., Cullen, D., Dauphin, P., Hamond, D., Hartmann, B. and Maynard, V., *Geochim. Cosmochim. Acta*, 1979, **43**, 1075-1090.
24. Murray, J. W., Balistrieri, L. S. and Paul, B., *Geochim. Cosmochim. Acta*, 1984, **48**, 1237-1247.
25. Bostrom, K., *Nature*, 1970, **226**, 629-630.
26. Wangersky, P. J. and Hutchinson, G. E., *Nature*, 1959, **181**, 108-109.
27. Borole, D. V., *Deep-Sea Res.* I, 1993, **40**, 761-775.
28. Chester, R. and Hughes, J. M., *Deep-Sea Res.*, 1969, **16**, 639-654.
29. Marchig, V. and Gundlach, H., in *La Genese des Nodules du Manganese*, Colloques Internatio naux du C N R S N, 1979, Vol **289**, pp. 55-60.
30. Banerjee, R. and Iyer, S. D., *Mar. Geol.*, 1991, **97**, 413-421.
31. Berger, W. H., Finkel, R. C., Killingley, J. S. and Marchig, V., *Nature*, 1983, **303**, 231-233.
32. Plueger, W. L., Friedrich, G. and Stoffers, P., *Monograph Series on Mineral Deposits*, Gebruder Borntraeger, Berlin, 1985, vol. 25, 31-52.
33. Gupta, S. M., *J. Paleon. Soc. India*, 1988, **33**, 59-71.
34. Wilson, T. R. S., Thompson, J., Colley, S., Culkin, F. and Sorensen, J., *Science*, 1986(a), **232**, 927-975.
35. Wilson, T. R. S., Thomson, J., Hydes, D. J., Colley, S., Culkin, F. and Sorensen, J., *Science*, 1986(b), **234**, 1129.
36. Wallace, H. E., Thomson, J., Wilson, T. R. S., Weaver, P. P. E., Higgs, N. C. and Hydes, J. D., *Geochim. Cosmochim. Acta*, 1988, **52**, 1557-1569.

ACKNOWLEDGEMENTS. I thank Mr S. M. Gupta for the faunal data. I am thankful to Mr R. R. Nair, Dr C. S. Murty, Prof. Supriya Roy and to my colleagues Mr. B. Nagendernath, Dr Dilip Kumur and Dr P. V. Narvekar for critical review. The research was carried out with financial support from the DOD under their programme on polymetallic nodules surveys.

Received 28 July 1993; revised accepted 12 August 1993

A comparative analysis of the molars of *Mus booduga*, *Mus dunnii* and fossil *Mus* of the Indian subcontinent: Phylogenetic and palaeobiogeographic implications

Rajeev Patnaik, Min Bahadur*, T. Sharma* and Ashok Sahni

Centre of Advanced Study in Geology, Panjab University, Chandigarh 160 014, India

*Centre of Advanced Study in Zoology, Banaras Hindu University, Varanasi 221 005, India

Upper molars of *Mus booduga* collected from Varanasi and *Mus dunnii* (chromosome type-I) show slightly derived features compared to those of *Mus booduga* collected from Mysore and *Mus dunnii* (chromosome type-II). *Mus auctor*, *Mus elegans*, *Mus flynnii*, *Mus sp. indet.*, *Mus jacobsi*, *Mus sp.*, *Mus booduga* and *Mus dunnii* are closely related to each other in having moderately elongated and rather strongly distorted M¹s and moderately reduced M³s (except for *Mus elegans*, *Mus sp.* and *Mus jacobsi*). Representation of *Mus*, both in terms of taxonomic diversity and considerable numbers, in the Plio-Pleistocene deposits of the Indian subcontinent is indicative of an early diversification event in the history of *Mus*.

IN all murids, M¹ (first upper molar) is relatively longer than M² (second upper molar), which in turn is longer than M³ (third upper molar). According to Misonne¹ lengthening of M¹ in a forward direction accompanied by reduction of M³, brings the whole series forward and occupies the place left by P⁴ (fourth upper premolar). The length of M¹ and M³ is given in relation to M², which has a standard relative length of 100% (ref. 1). Generally ancient murids have broad molars, thus Misonne¹ suggested that broad molars correspond to the more generalized types. Jacobs² proposed that in primitive murids, labial cingulum on lower molars are poorly developed and anterostyle on M¹ relative to lingual anterocone, but not on the posterior extremity.

During the preliminary studies on Late Pliocene *Mus*, it was observed that it resembles *Mus booduga*, the Indian Pigmy Field mice³, most closely. In the light of evolutionary trends of murids suggested by Misonne¹ and generalized dental characters of murids proposed by Jacobs² an attempt has been made here to study *Mus booduga* (extant taxon, collected from Varanasi and Mysore), *Mus dunnii* (extant taxon, chromosome types I, II and III), *Mus auctor* and *Mus sp.* reported from Late Miocene and Early Pleistocene Siwalik deposits, respectively², *Mus flynnii* and *Mus sp. indet.* recovered from Late Pliocene (around 2.5 m.y.) Siwalik sediments